

## GIANT PLANETS AROUND FGK STARS FORM PROBABLY THROUGH CORE ACCRETION

WEI WANG,<sup>1,2</sup> LIANG WANG,<sup>3,1</sup> XIANG LI,<sup>1</sup> YUQIN CHEN,<sup>1,4</sup> AND GANG ZHAO<sup>1,4</sup>

<sup>1</sup>*Key Laboratory of Optical Astronomy, National Astronomical Observatories, Chinese Academy of Sciences, Beijing 100101, China*

<sup>2</sup>*Chinese Academy of Sciences South America Center for Astronomy, National Astronomical Observatories, Chinese Academy of Sciences, Beijing 100101, China*

<sup>3</sup>*Max-Planck-Institut für Extraterrestrische Physik, Giessenbachstrasse, D-85748 Garching, Germany*

<sup>4</sup>*School of Astronomy and Space Science, University of Chinese Academy of Sciences, Beijing 100049, China*

### ABSTRACT

We present a statistical study of the planet-metallicity (P-M) correlation, by comparing the 744 stars with candidate planets (SWPs) in the Kepler field which have been observed with LAMOST, and a sample of distance-independent, fake “twin” stars in the Kepler field with no planet reported (CKSNPs) yet. With the well-defined and carefully-selected large samples, we find for the first time a turn-off P-M correlation of  $\Delta[\text{Fe}/\text{H}]_{\text{SWPs-SNPs}}$ , which in average increases from  $\sim 0.00 \pm 0.03$  dex to  $0.06 \pm 0.03$  dex, and to  $0.12 \pm 0.03$  for stars with Earth, Neptune, Jupiter-sized planets successively, and then declines to  $\sim -0.01 \pm 0.03$  dex for more massive planets or brown dwarfs. Moreover, the percentage of those systems with positive  $\Delta[\text{Fe}/\text{H}]$  has the same turn-off pattern. We also find FG-type stars follow this general trend, but K-type stars are different. Moderate metal enhancement ( $\sim 0.1 - 0.2$  dex) for K-type stars with planets of radii between 2 to 4  $R_{\oplus}$  as compared to CKSNPs is observed, which indicates much higher metallicities are required for Super-Earths, Neptune-sized planets to form around K-type stars. We point out that the P-M correlation is actually metallicity-dependent, i.e., the correlation is positive at solar and super-solar metallicities, and negative at subsolar metallicities. No steady increase of  $\Delta[\text{Fe}/\text{H}]$  against planet sizes is observed for rocky planets, excluding the pollution scenario as a major mechanism for the P-M correlation. All these clues suggest that giant planets probably form differently from rocky planets or more massive planets/brown dwarfs, and the core-accretion scenario is highly favoured, and high metallicity is a prerequisite for massive planets to form.

*Keywords:* stars: planetary systems - planets and satellites: formation - planets and satellites: general - techniques: photometric - techniques: spectroscopic - surveys

## 1. INTRODUCTION

The dependences of planet occurrence rate on host star properties provide important input for our understanding of planet formation and evolution, especially the well-known planet-metallicity (P-M) correlation as discovered by [Gonzalez \(1997\)](#) for giant planets, i.e., the planet occurrence is higher around metal-rich stars. This correlation may be the signature of self-pollution during the planet formation process (e.g. [Gonzalez 1997](#); [Murray et al. 2002](#); [Murray & Chaboyer 2002](#)), following the planet migration description of [Lin et al. \(1996\)](#), or indicates that high metallicity is a prerequisite for the formation of gas giants ([Fischer & Valenti 2005](#), e.g.), as demanded by the core accretion scenario (e.g. [Ida & Lin 2005](#)). We note that selection effects might be a third factor for the correlation at least for the studies concentrated on planets found via high-resolution spectroscopic radial velocity methods, where the sample of stars with planets is naturally biased to high metallicity and nearby bright stars. However, this effect is less significant for the samples with planets discovered through other techniques, e.g. the transit method.

The NASA *Kepler* mission ([Borucki et al. 2011](#)) has had great success in finding transiting exoplanet candidates. More than 3500 planet candidates have been discovered during its 4.5-year mission ([Batalha et al. 2013](#); [Burke et al. 2013](#)). This mission has a unique power to make it possible to study the planet occurrence rate and especially  $\eta_{\text{Earth}}$ , the fraction of Sun-like stars harboring Earth-like planets, in a reliable way. More importantly, the mission provides a high confidence for either the detection of planets (false positives  $\sim 7\% - 18\%$  depending on the radii of planets, [Morton & Johnson 2011](#); [Fressin et al. 2013](#); [Morton et al. 2016](#)) or the number of stars being searched but without known planets; The latter is guaranteed by the high precision and time coverage of *Kepler* photometry, which has never been achieved in the past. Afterwards, planet occurrence rate has been extensively studied ([Catanzarite & Shao 2011](#); [Howard et al. 2012](#); [Fressin et al. 2013](#); [Dressing & Charbonneau 2013](#)), and its dependency on metallicity (P-M correlation) has also been tackled, for example, by [Buchhave et al. \(2012\)](#), [Everett et al. \(2013\)](#), [Wang & Fischer \(2013\)](#), [Buchhave et al. \(2014\)](#) and [Schlaufman \(2015\)](#).

[Buchhave et al. \(2012\)](#) measured precise stellar parameters and metallicity [m/H] for a sample of 152 *Kepler* planet-host stars using their stellar parameters classification (SPC) tool (Supplementary information of [Buchhave et al. 2012](#)). They used a set of high-resolution low-to-moderate ( $\sim 13 - 312$ ) SNR echelle spectra, and fit them in the wavelength ranged between 5050 and 5360 Å to a library grid of synthetic model spectra. They found a positive correlation between the planet occurrence rate and stellar metallicity for giant planets, i.e., the planet-metallicity (P-M) correlation. However, the metal-

licity pattern for stars hosting planets with radii smaller than  $4R_{\oplus}$  does not clearly reveal any correlations. Instead, a wide range of metallicity distribution was observed in their sample. [Everett et al. \(2013\)](#) derived stellar parameters and [Fe/H] for 220 faint *Kepler* planet candidate host stars, by fitting model spectra published by [Coelho et al. \(2005\)](#) to moderate-resolution ( $R \sim 3000$ ) optical spectra covering 3800 – 4900 Å. They concluded that the frequency of large planets in the sample depends on host star metallicity, similar to that found for the sample of brighter KOI stars by [Buchhave et al. \(2012\)](#). Later on, by employing stellar and orbital parameters from the KOI website<sup>1</sup>, and stellar metallicities from *Kepler* Input Catalog (KIC, [Brown et al. 2011](#)), [Wang & Fischer \(2013\)](#) investigated this question in a better sample including only multi-planet systems which are claimed to have a substantially lower false positive rate ([Lissauer et al. 2012](#)). They confirmed the positive P-M correlation for gas giant planets with radius between  $5R_{\oplus}$  and  $22R_{\oplus}$ , and it holds for Neptune-size planets with radius between  $2R_{\oplus}$  and  $5R_{\oplus}$ , however not for Earth-sized planets with radius less than  $2R_{\oplus}$ . [Buchhave et al. \(2014\)](#) used the same method to derive stellar parameters for 405 stars orbited by 600 exoplanet candidates, and they claimed that the planets can be categorised into three regimes defined by statistically distinct metallicity regions, reflecting the different formation scenarios of rocky planets, gas dwarf planets and gas/icy giant planets.

More recently, [Wang & Fischer \(2015\)](#) and [Buchhave & Latham \(2015\)](#) used a same sample of 405 stars with transiting planets but different reference stellar samples to explore the P-M correlation. While [Wang & Fischer \(2015\)](#) used a sample of Solar-like *Kepler* stars with no known planets as the reference sample, [Buchhave & Latham \(2015\)](#) employed the 518 dwarf stars from the asteroseismic sample ([Chaplin et al. 2014](#)) for comparisons. Interestingly and instructively, the former exercise detected the P-M correlation for terrestrial planets, while the later reported a null detection for them. This indicates it is crucial to choose and refine an appropriate and unbiased reference sample, and to have reliable or at least consistent determinations of stellar metallicities.

We note that in [Wang & Fischer \(2013\)](#), the stellar metallicity [Fe/H] is taken from *Kepler* Input Catalog (KIC, [Brown et al. 2011](#)), which is known to be of large uncertainties of  $\sim 0.4$  dex, and is recently found to underestimate both the true metallicity and dynamic range ([Everett et al. 2013](#); [Dong et al. 2014](#)), thanks to Data Release 1 (DR1, [Luo et al. 2012](#)) of the Large Sky Area Multi-Object Fiber Spectroscopic Telescope (LAMOST, a. k. a., Guoshoujing telescope, [Cui et al. 2012](#); [Zhao et al. 2012](#)). In 2016, LAM-

<sup>1</sup> <http://exoplanetarchive.ipac.caltech.edu>

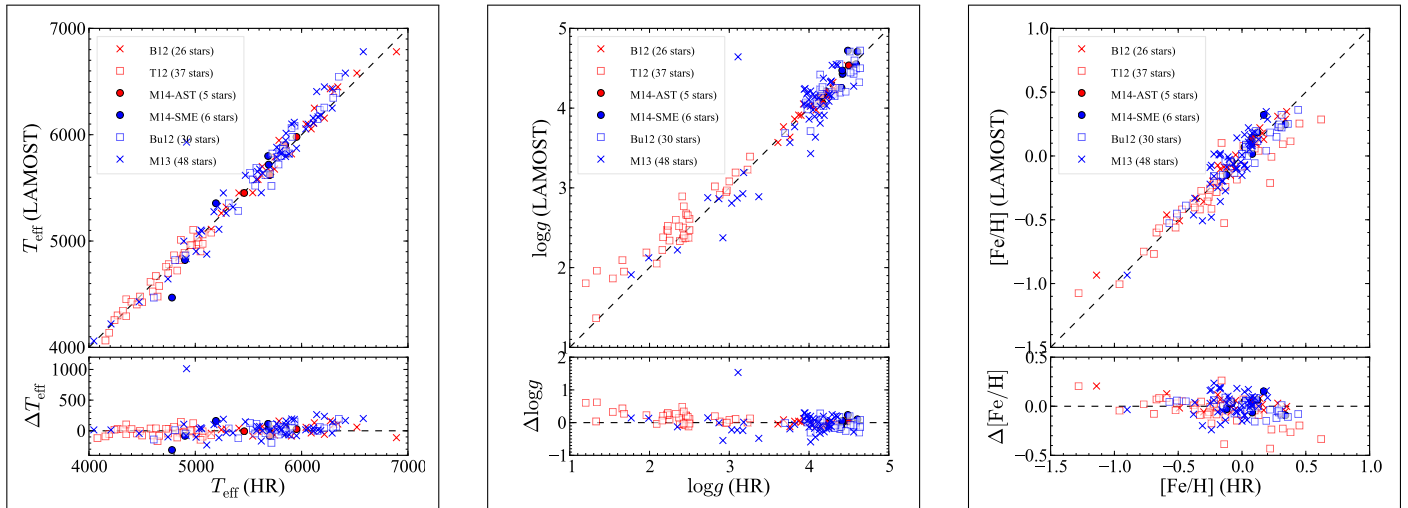


**Figure 1.** Comparisons of  $T_{\text{eff}}$  (Left) and  $[\text{Fe}/\text{H}]$  (Right) between those from LAMOST DR3 and those from recent high-resolution spectroscopic studies by Bruntt et al. 2012, Thygesen et al. 2012, Molenda-Żakowicz et al. 2013, Buchhave et al. 2012, Marcy et al. 2014.

OST DR3 (hereafter LMDR3) has been released, includes 3,177,995 FGK-type stars with stellar atmospheric parameters (APs) automatically determined consistently using the LAMOST Stellar Parameter Pipeline (LSPP, Wu et al. 2011), at precisions of 110 K, 0.19 dex and 0.11 dex for stellar effective temperature  $T_{\text{eff}}$ , gravity  $\log g$  and metallicity  $[\text{Fe}/\text{H}]$ , respectively (Wu et al. 2014). We further examined LSPP  $T_{\text{eff}}$  and  $[\text{Fe}/\text{H}]$  with those determined from high resolution spectroscopic data in three recent work (Bruntt et al. 2012; Thygesen et al. 2012; Molenda-Żakowicz et al. 2013), and found a good agreement with a median discrepancy of  $-36 \pm 108$  K in  $T_{\text{eff}}$  and  $-0.02 \pm 0.11$  dex in  $[\text{Fe}/\text{H}]$ , as seen in Fig. 1. In Wang et al. 2016, we made an extensive study of the  $\log g$  determinations from LSPP and those from asteroseismology with the Kepler data, and performed a calibration of the former with the latter. We surprisingly found that LSPP gives quite robust internal  $\log g$  in the sense that by applying a piecewise linear functions of the difference between LSPP  $\log g$  and asteroseismic  $\log g$  against LSPP  $T_{\text{eff}}$ , the residual has a close-to-zero mean value of  $-0.02$  and a standard deviation of merely 0.13 dex, with only 3% outliers. In summary, the error budget for LSPP APs are 108 K, 0.13 dex and 0.11 dex for  $T_{\text{eff}}$ ,  $\log g$  and  $[\text{Fe}/\text{H}]$ , respectively. LMDR3 includes about 68,764 Kepler stars as part of the “LAMOST-Kepler project”, which aims to combine these two unique surveys together for various studies including planetary science and stellar physics, i.e., Kepler provides high quality photometry and light curves for the studies of stellar asteroseismology and transit planets, while LAMOST can provide relatively reliable and self-consistent atmospheric parameters (APs) for the stars rapidly.

With the emergence of the large data set of medium-resolution spectra produced by LAMOST, several investigations come up very recently with quite interesting results.

Employing the LAMOST-Kepler data set, Mulders et al. (2016) studied the dependences of the P-M correlation on orbital period and planet size, and found that planets with orbital periods less than ten days are more likely detected around metal-rich stars, and this trend is most significantly for rocky planets. Dong et al. (2018) discovered a population of short-period, Neptune-sized planets, which are similar to hot Jupiters in the aspects that they are both preferentially orbiting metal-rich stars as revealed by LAMOST, and are both in the mean time preferentially single-transiting planetary systems as observed by Kepler.

In this study, we present our results using the “LAMOST-Kepler project” to study the planet-metallicity correlation. We will show in Section 2 how reliable the stellar parameters given in LMDR3 are. In Section 3, we will introduce the target sample of 744 Kepler stars with detected candidate planets (SWPs) and two control samples bKSNP and CK-SNP, and will discuss them in details in Section 4. A brief summary will be given in the last section.

## 2. THE TARGET SAMPLE AND THE CONTROL SAMPLES

We cross checked LMDR3 with Kepler candidate catalogue and Exoplanet Data Explorer (<http://exoplanets.org>, hereafter EDE, Han et al. 2014), and found 801 stars harbouring in total 1045 planets. They are targeted as field stars in LAMOST Experiment for Galactic Understanding and Exploration (LEGUE) survey (Deng et al. 2012), and the LAMOST-Kepler project (De Cat et al. 2015). We restrain the sample into dwarf stars with  $\log g > 3.5$ , to avoid any possible metal contaminations during the late stellar evolutionary stages in (sub)giant stars. We further remove the KOI 607 system, because recently the companion is found to be a low-mass star instead of a planet or brown dwarf, with  $M = 0.106 \pm 0.006 M_{\odot}$  measured through 2 high-precision

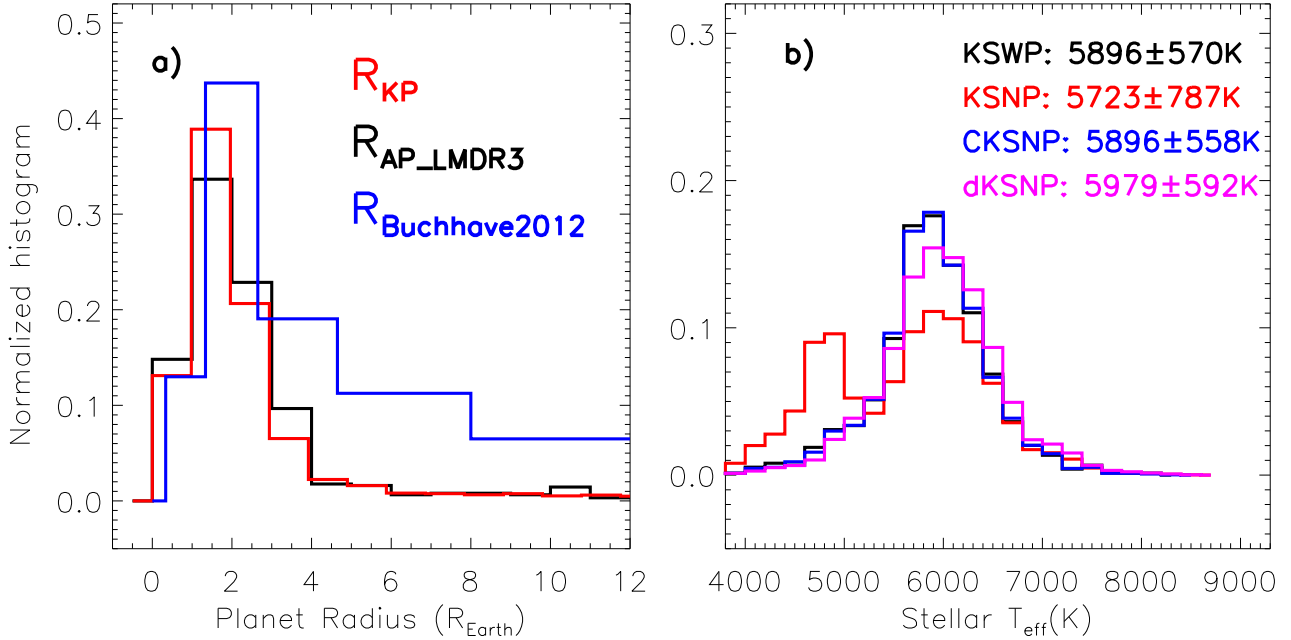


**Figure 2.** The distribution of planet radius (Left) and stellar effective temperature  $T_{\text{eff}}$  (Right). Left: red histogram for all *Kepler* candidate planets, black for all planets from EDE found in LAMOST DR3, blue for the planets in [Buchhave et al. \(2012\)](#); Right: median values and standard deviations of  $T_{\text{eff}}$  for every samples are marked. The purple histogram is the distribution of  $T_{\text{eff}}$  of dwarf KSNPs with  $\log g > 3.5$ .

velocimetry measurements ([Santerne et al. 2012](#)). Among the rest, there are 744 *Kepler* stars with SDSS  $g$  and  $r$  magnitudes reported in literatures, this assembles the **SWP** sample. The planets around stars in this sample are mostly candidate Super-Earths or Neptunes. It has a size distribution very similar to that of the entire *Kepler* candidate planet sample, as shown in Fig. 2. In contrast, the size distribution of candidate planets in [Buchhave et al. \(2012\)](#) is obviously different from the entire *Kepler* planet sample (the blue histogram compares the red in Fig. 2); their sample includes slightly smaller fraction of planets with radii below  $1.3R_{\oplus}$  ( $\sim 25\%$ ), and much higher fraction (a factor of  $\sim 2$ ) of planets with radii larger than  $4R_{\oplus}$ .

There are **67,787** *Kepler* stars with no known planets that have spectra taken by LAMOST and released in DR3. These stars form a control SNP sample, named as **KSNP**. However, we stress that for such investigations, KSNP is not a well-defined control sample. In Fig. 2b, distributions of  $T_{\text{eff}}$  given by LSPP are plotted for the target SWP sample and the three control samples. There is a clear deviation of the distributions of SWP (black) and KSNP (red) at lower stellar  $T_{\text{eff}}$ , especially at  $T_{\text{eff}} < 5300$  K. Further investigations show that about 78% of KSNPs within this  $T_{\text{eff}}$  regime are giants or sub-giants with  $\log g < 3.5$ , and only  $\sim 22\%$  of SWPs are not dwarfs. If we remove all KSNPs with  $\log g < 3.5$  (the purple histogram), the large difference at  $\sim 5000$  K disappears. It is not unexpected given that all the planets under current study were found using the transit method, with

which the detection rates are highly dependent on the stellar radius, and therefore largely different for giant and dwarf stars. Additionally, giants and dwarfs have statistically different metallicity distributions. We note that thus cautions should be made for a clean selection of the control sample for the study of the P-M correlation, but has never done well enough in any previous studies.

The best way to tackle the P-M correlation is to compare a sample of twin stars, with one of the twin hosting planets while the other not. In this case, the presence of planets is the only cause of metal enrichment, or the only result of high metallicity. To approach this, we assemble a control sample consisting of “composite twin” stars, to minimize possible influences induced by  $T_{\text{eff}}$ ,  $\log g$  and stellar distance ( $D$ ), and to study a “clean” P-M relationship. For each of the 744 planet-host stars, we chose from the KSNP sample 9 reference stars, which are the most similar to the target star, but with no known planets. In practice, the difference between SWP and their reference stars is represented using the distance in the ( $T_{\text{eff}}$ ,  $\log g$ , dereddened  $r$  magnitude) 3-D parameter space for each SWP and its counterparts. The units for these three quantities are 100 K, 1 dex, 1 mag for the parameter space distance calculations. The stars with the smallest distances and with  $r$ -band signal-to-noise ratio (SNR) higher than three were chosen. Such kind of selection process naturally results in a very similar distribution of  $T_{\text{eff}}$  (Fig 2b.),  $\log g$  and the dereddened  $r$ -band magnitude of SWPs and SNPs. These similarities will consequently lead to similar-

ities in stellar mass ( $M$ ), radius ( $R$ ) and stellar distance to first-order approximation if metallicities do not differ significantly, as well as detection rates of planets. The total 6696 analog stars selected from LMDR3 Kepler field stars assemble the “best” Kepler SNP (bKSNP) sample.

For each SWP, a comparison fake star is “created” in AP space, with APs using the median values of the nine most similar KSNPs. The “composite” fake star and its corresponding SWP are therefore star analogs or star twins, according to the definitions of solar twins and solar analogs (Soderblom & King 1998). These 744 fake analog stars assemble the CKSNP sample, which will be used in the following analysis. We further check the differences of SWPs and CKSNPs in 2MASS color spaces, namely  $J - H$ ,  $H - K_s$  and  $J - K_s$ . The differences in the three colors are mostly smaller than 0.1 mag, with standard deviations 0.04, 0.03 and 0.05 mag, respectively. The small discrepancies in 2MASS colors provide independent support to the similarities of SWP and CKSNP stars. We show in Fig.3 the differences of  $T_{\text{eff}}/100$ ,  $\log g$  between SWP and its corresponding twin-like composite SNP. Most of these pairs have differences  $< 10$  K in  $T_{\text{eff}}$ , and 0.1 dex in  $\log g$ . On the other hand, obvious deviations of  $[\text{Fe}/\text{H}]$  distributions in these two samples do exist, as shown by the red circles and more clearly in the red histogram Fig.3. At first glance, there is no clear evidence for metal enrichments of SWPs compared to SNPs as a bulk, given their very small difference ( $-0.00 \pm 0.001$  dex) of the mean  $[\text{Fe}/\text{H}]$  values. However, the red circles in the left panel shows clearly how the  $[\text{Fe}/\text{H}]$  discrepancy in the two samples evolve interestingly with SEQ, which is representing the increasing indices of  $[\text{Fe}/\text{H}]_{\text{SWP}}$ . Further discussions about this issue will be presented in Section 3.

We emphasize here the stellar distance is an important parameter that should be taken into account but previously ignored when selecting control sample. Because if we change the parameter distance between SWP and SNP samples in the  $r$  magnitude space from 2, 1 to  $-1$  and  $-2$ , i.e., the control sample stars are further and further away from us, the mean  $[\text{Fe}/\text{H}]_{\text{bKSNP}}$  steadily decreases from  $-0.01$ ,  $-0.03$  to  $-0.06$  and  $-0.07$ , accordingly (Fig. 4), in which it is clearly shown that this trend is also true for each  $T_{\text{eff}}$  bin. We emphasized here that one must be very careful with the selection of control samples for the study of the P-M correlation and plane frequency. With an inappropriate control sample, an inadequate, or wrong conclusion might be drawn. In our case,  $\sim 97\%$  of the bKSNP star have a  $r$  mag difference from that of SWP within 0.25 mag, and  $\sim 79\%$  of them within 0.10 mag, which corresponds to a difference of 12% and 5% in distance assuming a same stellar intrinsic luminosity, respectively. Therefore, for each SWP, its corresponding 9 bKSNP reference stars are very nearby and similar stars,

and thus much suitable for such a study, when compared with other similar investigations.

The same exercise is also carried out for the entire LMDR3 SNP sample (LSNP), consisting of about 1 million stars. We find a significant and positive large metallicity enhancements ( $\sim 0.20 \pm 0.01$  dex) of SWPs compared with LSNPs. Then we realize that this might be a result of the fact that the Kepler field stars without planets are already generally metal-rich than those in other Galactic fields (cf. for example Dong et al. 2014), which means it is better to use control stars in the Kepler field to eliminate the metallicity-spatial-variation bias, as done in this work.

In the following, our discussion and conclusions will be mostly based on the comparative analysis between SWP and CKSNP (the “composite” Kepler SNP sample). We prefer CKSNP to dKSNP (the dwarf KSNP sample as shown in purple curve in 2). The main reason is that CKSNP and SWP stars have similar  $T_{\text{eff}}$  and  $\log g$ , and therefore the LSPP should in principle give similar systematics and uncertainties in the determinations of  $[\text{Fe}/\text{H}]$ , and therefore comparing them will be more self-consistent and homogeneous. Another major reason is that CKSNP and SWP have very similar stellar distance, making them possible to have same origins and therefore similar initial metallicities.

### 3. DISCUSSION

SWPs with giant planets have averagely higher metallicities than SNPs, as observed, for example, by Fischer & Valenti (2005), Neves et al. (2013), and as interpreted by the core accretion planet formation theory (Ida & Lin 2004; Ercolano & Clarke 2010). Such positive relationship between planet occurrence rate and stellar metallicity becomes partially vanish for stars hosting Neptunian-sized and even smaller planets (e.g. Sousa et al. 2008; Bouchy et al. 2009; Ghezzi et al. 2010; Sousa et al. 2011; Buchhave et al. 2012; Adibekyan et al. 2012). Fig. 5 shows the  $[\text{Fe}/\text{H}]$  distributions for SWPs (the red histogram) and CKSNPs (the black one) and bKSNPs (the blue one). The SWP, CKSNP and bKSNP samples samples have mean  $[\text{Fe}/\text{H}]$  values of  $\sim -0.03 \pm 0.008$ ,  $\sim -0.05 \pm 0.008$  and  $\sim -0.05 \pm 0.003$  dex, respectively, where the error bars are standard errors of the means. We conclude that there is not significant difference between the SWP and SNP samples, as shown by the red and blue histograms and the one-component Gaussian-fitting curves in the plot. Given the fact that most (80%) of our SWPs harbor planets of  $R_p < 5R_{\oplus}$ , the observed similar metallicity suggests that stars with Neptune-sized and Earth-sized planets might not be distinguishable from those without known planets. This discovery seems to be in line with the conclusion drawn by Buchhave et al. (2012) and is different from Wang & Fischer (2015) and Adibekyan et al. (2012). The latter authors carried out a uniform and detailed abun-

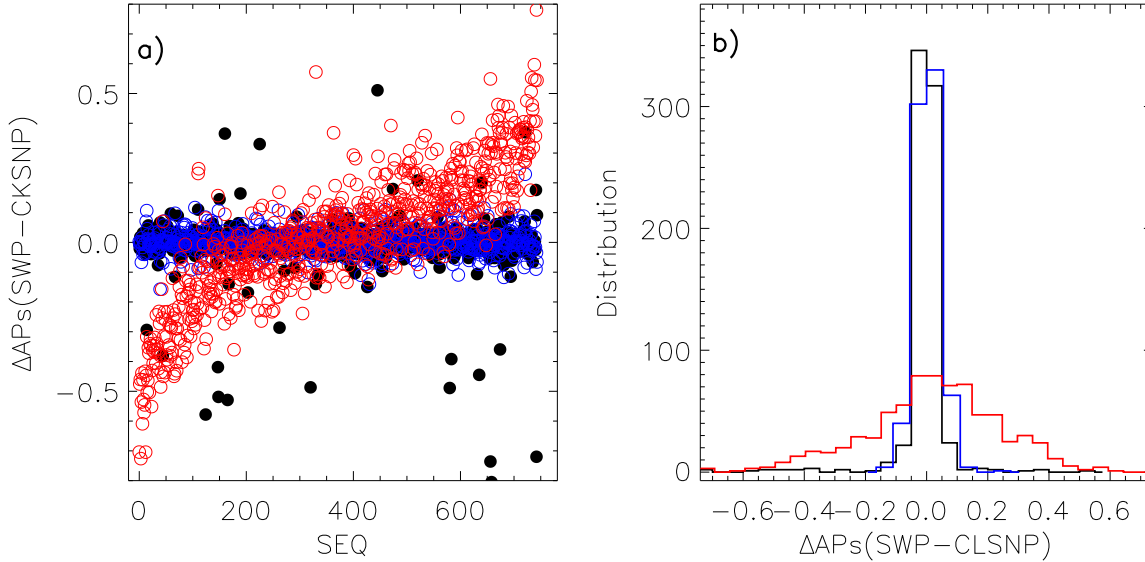


**Figure 3.** The differences of  $T_{\text{eff}}/100$ ,  $\log g$  and  $[\text{Fe}/\text{H}]$  between SWPs and CKSNPs in blue, black and red, respectively, shown as scatter points with increasing SWP metallicity in the left panel and histogram in the right panel. The horizontal axis in the left panel, SEQ, is the sequence of the SWP stars in order of increasing metallicity. The mean values of these differences are, respectively,  $-0.5$  K,  $0.003$  and  $0.02$  dex.

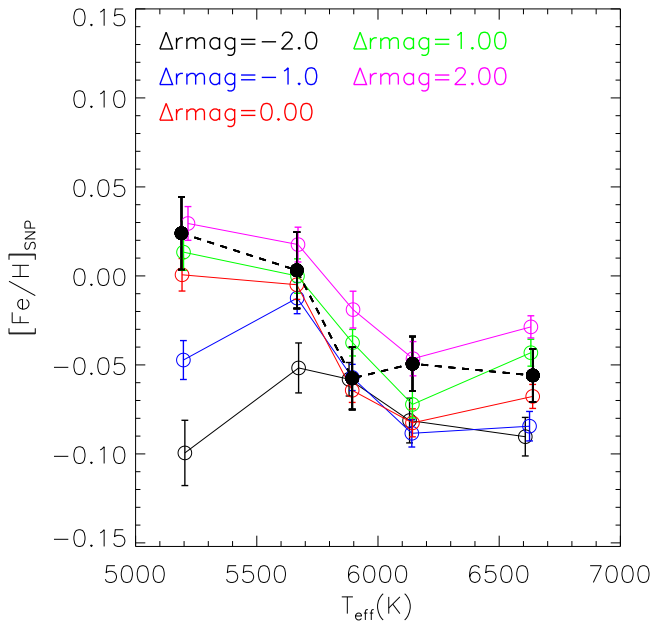


**Figure 4.** Average  $[\text{Fe}/\text{H}]$  in various  $T_{\text{eff}}$  bin as a function  $T_{\text{eff}}$ . The black dashed line represents for SWPs, and the solid lines for CKSNPs with  $\Delta r$  from  $-2.0$  to  $2.0$  mag, respectively.

dance analysis of 12 refractory elements for a sample of 1111 FGK dwarf stars from the HARPS GTO planet search program and found that the 26 Neptunian/super-Earth hosts have

average  $[\text{Fe}/\text{H}]$  value  $\sim 0.23$  dex lower than Jovian hosts, and  $\sim 0.04$  dex higher than Non-planet hosts.

Although the P-M correlation is not observed with high significance when comparing in general our target and control samples, we will show in the following three subsections that the so-called P-M correlation is evidently shown. In addition, we find that the P-M correlation is dependent to planet radius, stellar metallicity and stellar spectral types. The first dependency, i.e., different P-M correlation at different planet radius, has been reported and discussed extensively previously, but the last two dependencies are both firstly reported in the current study.

### 3.1. The P-M correlation is confirmed to depend on the planetary radius

In Fig. 6, we plot  $\Delta[\text{Fe}/\text{H}] = [\text{Fe}/\text{H}]_{\text{SWP}} - [\text{Fe}/\text{H}]_{\text{CKSNP}}$  against planet radius  $R_{\text{P}}$  in units of Earth radius ( $R_{\oplus}$ ) using the black filled circles for the 744 SWP-CKSNP pair. Cyan points with error bars represent the average  $[\text{Fe}/\text{H}]$  in each uneven bin, grouped in 1, 2, 3, 4, 9, 22, and  $500R_{\oplus}$ , which clearly shown a turn-off trend, peaking at  $\sim 9R_{\oplus}$ . The bin size is indicated by the width of the shaded grey histogram, and the histogram represents the number of targets in each bin scaled by the right-side Y-axis. It is clearly seen that the mean  $\Delta[\text{Fe}/\text{H}]$  values are close to zero for SWEPs (stars with Earth-sized planets) with  $R_{\text{P}} < 2R_{\oplus}$ , increase to  $\sim 0.03$  dex for stars with Super-Earths with  $2R_{\oplus} < R_{\text{P}} < 4R_{\oplus}$ , and to  $0.07 \pm 0.03$  for SWNPs (stars with Neptunian-

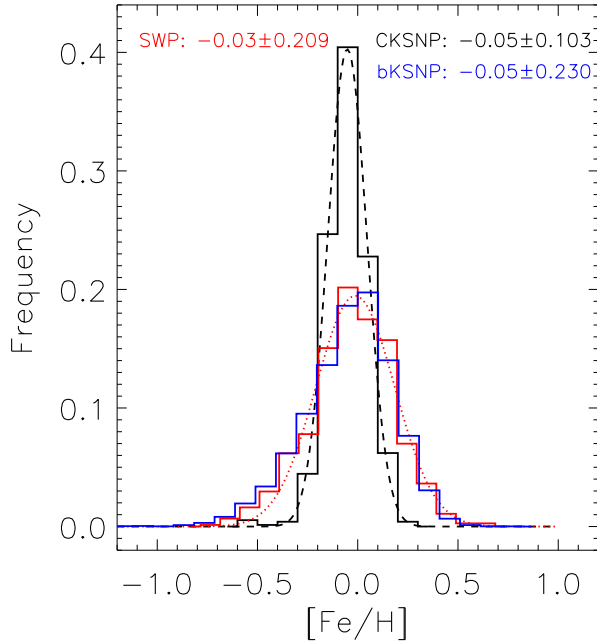


**Figure 5.** The histogram of  $[\text{Fe}/\text{H}]$  of CKSNPs (black), bKSNP (blue) and SWPs (red). The black and red over-plotted dashed lines are one-component Gaussian fits to the distributions of  $[\text{Fe}/\text{H}]_{\text{CKSNP}}$  and  $[\text{Fe}/\text{H}]_{\text{SWP}}$ , respectively. The mean metallicities and their standard error of mean of each sample are shown in the plot.

sized planets) with  $4R_{\oplus} < R_{\text{P}} < 9R_{\oplus}$  and becomes evidently positive ( $0.12 \pm 0.03$ ) for SWJPs (stars with Jupiter-sized planets) with  $9R_{\oplus} < R_{\text{P}} < 22R_{\oplus}$ , and turns nearly zero ( $0.02 \pm 0.03$ ) for even larger planets or brown dwarfs. We note that the same turn-off pattern still holds for our data set, if  $[\text{Fe}/\text{H}]_{\text{SWP}}$ , instead of  $\Delta[\text{Fe}/\text{H}]$ , is to be plotted and compared. This is can be well explained by the fact that  $[\text{Fe}/\text{H}]_{\text{CKSNP}}$  is more narrowly distributed compared to  $[\text{Fe}/\text{H}]_{\text{SWP}}$ . Furthermore, it seems that SWJPs have a high possibility to be metal-enriched, i.e., with  $\Delta[\text{Fe}/\text{H}] > 0$ . We calculate the fraction of metal-enriched SWPs ( $f$ ) in each radius bin, and the resulting percentage is shown as the purple dots in Fig. 6. For reference, the percentage of 50% is shown as the dotted horizontal line. It is clearly shown that SWJPs and SWNPs are both likely ( $74 \pm 17\%$  &  $58 \pm 12\%$ ) to be metal-enriched, while  $\sim 55 \pm 10\%$  SWEs are metal-enriched, and only  $53 \pm 11\%$  stars with huge planets/brown dwarfs are metal-enriched. Again, the fraction  $f$  shows a clear turn-off pattern, which peaks at Jupiter size as well.

These turn-off patterns have not been reported yet, as the exercise extending companion’s radius to far beyond Jupiter’s radius has not been conducted in the past. We are aware those very large companions are probably not plan-

ets, and the purpose to include them in the current analysis is mainly to help our understanding of formation of planets larger than the Jupiter, and the difference of the giant planet formation and brown dwarf formation. This overall trend confirms that the P-M correlation is strong and positive for Jupiter-size planets, and is weakened for Neptune-size planets (Fischer & Valenti 2005; Sousa et al. 2011), and however contrary to the conclusions from some other works (e.g. Wang & Fischer 2015). On the other hand, this also suggests that the P-M correlation might have disappeared for Earth-sized planets and for much bigger planets/brown dwarfs. In summary, the P-M correlation is dependent on planet radius  $R_{\text{P}}$ .

We admit that the KSNP sample is not clean, because only those planets with small inclination angles can be detected with the transit method. Therefore in the KSNP sample, there should be noticeable “false” SNP stars actually hosting planets. To give a rough estimate of the False Alarm Possibility of SWPs in the KSNP sample, we adopt the average number of planets per star for different periods ranges for per planet size bin listed in Table 3 of Fressin et al. (2013). We estimate that for stars with large planets ( $R_{\text{P}} > 4R_{\oplus}$ ), the fraction of SWPs in the KSNP sample is no more than 6 percent. Taking into account a maximum metal enrichment of  $\sim 0.2$  dex for large planets, they should not increase the mean metallicities in each radius bin by more than 0.012 dex. For stars with small planets ( $R_{\text{P}} < 4R_{\oplus}$ ), this FAP can be as high as 31%. However, the resulting increase of mean metallicities should be smaller than 0.016 dex, given the currently measured metal enrichment of no more than  $\sim 0.05$  dex. Considering that both 0.012 dex and 0.016 dex are smaller than the error bars given in Fig. 4, 6 & 9, the pattern obtained from the uncleaned KSNP sample remain in principal untouched.

We point out that for the SWP sample, most planets are identified by the Kepler mission as planet candidates, or referred to as Kepler Objects of Interests (KOIs) from their periodic transit-like light curves. Previous investigations including, for example, Fressin et al. (2013) and Morton et al. (2016) show that the FAP (False Alarm Possibility) is about 7-9% for Kepler candidates with  $R_{\text{P}} < 4R_{\oplus}$ , and is about 16-22% for candidates with  $R_{\text{P}} > 4R_{\oplus}$ . Which means that for KOIs,  $\sim 8\%$  or  $19\%$  of them are actually not planetary systems, and they should be re-classified as stars without planets. For SWPs with  $R_{\text{P}} > 2R_{\oplus}$ , the P-M correlation is observed to be positive, and therefore wrongly including SNPs in our SWP sample will only make the metal enhancement less significant by  $\sim 20\%$ , or  $\sim 0.1$  dex. For the case of SWEs, i.e.,  $R_{\text{P}} < 2R_{\oplus}$ , the extent of over-metallicity is not significant, and therefore we can not tell which direction the false alarms would affect, but given the FAP of 8%, the resulting bias should not be noticeable.

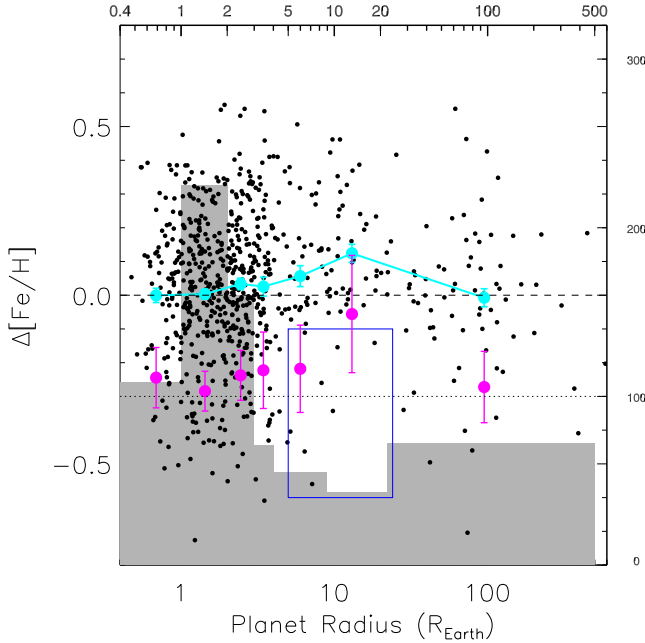


**Figure 6.**  $\Delta[\text{Fe}/\text{H}]$  against  $R_P$  in units of  $R_\oplus$  for the 744 comparison pairs (black dots). The mean and standard error of  $\Delta[\text{Fe}/\text{H}]$  in each of the 6 planetary radius bin are plotted in cyan symbols with error bars. The shaded grey histogram shows the number of planets in each bin. The blue box indicates a region that lack of stars with  $4R_\oplus < R_P < 24R_\oplus$ , and  $\Delta[\text{Fe}/\text{H}]$  between  $-0.6$  and  $-0.1$  dex. The purple dots with error bars give the percentages and their statistical uncertainties of metal-rich SWPs.

### 3.2. The P-M correlation is found to depend on stellar metallicity!

It has been investigated and discussed for a long time about the dependence of the P-M correlation on  $R_P$ . However, it has never been reported that the P-M correlation also depends on other stellar or planetary parameters. When playing with our SWP-CKSNP comparison sample, we find it quite interesting from Fig.7 that  $\Delta[\text{Fe}/\text{H}]$  shows a positive linear correlation with  $[\text{Fe}/\text{H}]_{\text{SWP}}$  with a slope of  $0.93 \pm 0.02$  and intercept of  $0.05 \pm 0.004$ , which has never been reported previously. The non-unity slope and marginally positive intercept support the fact that SWP is statistically slightly metal rich than CKSNP at solar metallicity, and the metal enhancement is quite significant at super-solar metallicity and becomes negative at subsolar metallicities. This suggests that the so-called P-M relation reported previously is in fact metallicity-dependent, and it is only valid for solar and super-solar metallicity stars. We realize that this relationship also holds if the whole sample is divided into three subsamples with different sizes of planets. Linear regressions of the SWJPs (purple triangles), SWNP (blue crosses) and SWEP (red diamonds) subsamples yield quite similar correlation coefficients, ranging from 0.92 to 0.95 for the slopes, and 0.04 to 0.06 for the intercepts. We note SWJPs are mostly having higher  $[\text{Fe}/\text{H}]$

and SWNPs with median values, while SWEPs with lower values.

The linear relationship might be a mathematical result from the fact that  $[\text{Fe}/\text{H}]_{\text{SWP}}$  has a larger dispersion ( $\sim 0.21$  dex), as compared to that of  $[\text{Fe}/\text{H}]_{\text{CKSNP}}$  ( $\sim 0.10$  dex), as clearly shown in Fig. 8 and Fig. 5. In the former figure,  $[\text{Fe}/\text{H}]_{\text{SWP}}$  (the black connected line) and  $[\text{Fe}/\text{H}]_{\text{CKSNP}}$  (the black scatter dots) are plotted one by one, as a function of the  $[\text{Fe}/\text{H}]_{\text{SWP}}$ . It is clear that  $[\text{Fe}/\text{H}]_{\text{SWP}}$  increases steadily from about  $-0.7$  to  $0.65$  dex, while  $[\text{Fe}/\text{H}]_{\text{CKSNP}}$  is nearly flat around zero metallicity, and is mostly between  $-0.25$  and  $0.20$  dex. The blue line is the least-square linear fit to  $[\text{Fe}/\text{H}]_{\text{CKSNP}}$  as a weak function of  $[\text{Fe}/\text{H}]_{\text{SWP}}$ , giving a hint that the former increases slowly with the latter. To make sure that this conclusion is not affected by data uncertainties, we create a new set of  $[\text{Fe}/\text{H}]_{\text{CKSNP}}$  by increasing the deviations of  $[\text{Fe}/\text{H}]_{\text{CKSNP}}$  around their local average values by a factor of two. Then we perform similar regression exercise to the new set of  $[\text{Fe}/\text{H}]_{\text{CKSNP}}$ , and we find similar although weaker linear correlations, which suggests that the observed linear relationship is more likely to be real.

No matter whether this linear relationship is a mathematical consequence or not, the key point and more fundamental character shown in our samples is that  $[\text{Fe}/\text{H}]_{\text{SWP}}$  has a larger variation, while  $[\text{Fe}/\text{H}]_{\text{CKSNP}}$  does not. We point out that as all the CKSNP stars are selected from within the Kepler field, it is quite reasonable that their metallicities are narrowly distributed. On the other hand, SWP stars have metallicities higher than their counterparts by various extent mainly related to various  $R_P$  and host stars' spectral type, and therefore have significantly larger variations. This obvious difference in the variations of  $[\text{Fe}/\text{H}]$  for SWPs and SNPs, and the strong correlation of  $\Delta[\text{Fe}/\text{H}]$  against  $[\text{Fe}/\text{H}]_{\text{SWPs}}$  evidently suggest that the Planet-Metallicity correlation (if exists) is metallicity-dependent, which is positive at high metallicities (solar and super solar), and becomes negative for subsolar metallicities.

We note that  $\Delta[\text{Fe}/\text{H}]$  are dependent both on  $[\text{Fe}/\text{H}]$  and on  $R_P$  is not a surprise, given the fact that most SWJPs which have large  $\Delta[\text{Fe}/\text{H}]$  locate mostly in the upper-right portion in Fig.7. This turn-off trends of  $\Delta[\text{Fe}/\text{H}]$  and  $f$  against  $R_P$  indicates that the gas giant planets are different from rocky planets and brown dwarfs, in the aspect of the metallicities of their host stars, and thus implies a different mechanisms and requirements for the formation of gas giants, compared to rocky planets, and to more massive planets/brown dwarfs. This implication naturally excludes the disk instability scenario for gas giant formation.

We should make another statement that, the metal pollution scenario, i.e., host stars engulfing migrating planets into their photospheres and therefore enrich their apparent

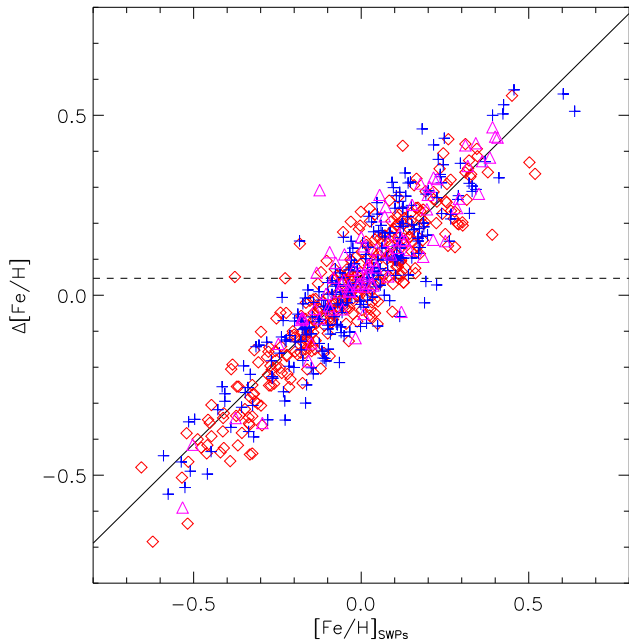


**Figure 7.**  $\Delta[\text{Fe}/\text{H}]$  against  $[\text{Fe}/\text{H}]_{\text{SWPs}}$ . The solid line represents the best-fit curve with a slope of  $0.93 \pm 0.02$  and intercept of  $0.05 \pm 0.004$  respectively. The dashed line shows the intercept of the best fit. Red diamonds, blue crosses and purple triangles represent SWEs, SWNPs and SWJPs, respectively.

metallicity, can not be the only reason for the P-M correlation for SWJPs. Metallic material of  $5 - 10 M_{\oplus}$  from rocky planets or giant planets are believed to be enough to enrich the apparent photospheric metallicities by about 0.1 dex for G-type stars, more for earlier type stars and less for later type stars, depending on the mass of their photospheric layers (Gonzalez 1997). In this scenario, massive rocky planets should have similar although less-serious pollution, and  $\Delta[\text{Fe}/\text{H}]$  should increase with  $R_{\text{P}}$  because larger planets should contain more metals. The first four red and purple dots in Fig. 6 are almost identical within error bars, and there is only marginal ascending trend observable and therefore our data set does not support this metal pollution scenario. More accurate measurements of  $[\text{Fe}/\text{H}]$  should help to better constrain this trend for our sample.

Moreover, we argue that the higher metallicity is a requirement for gas giants to form, but not necessary for rocky planets and brown dwarfs. This is supported by the obvious deficit of SWJPs in the blue box region in Fig. 6, and the high  $f$  of SWJPs and SWNPs. Just to mention, the 7 SWPs that have modestly low metallicity worth future high-resolution study, which might be helpful for the understanding of how planets form in metal-poor environments. We note that it is not necessary at all to be metal-rich to form small planets, arguing against the theoretical requirement of  $[\text{Fe}/\text{H}] > 0.3$  to bear terrestrial planets (Gonzalez et al. 2001). In other words,

the birthplace of terrestrial planets might be widespread in the Galaxy, and even possible back to the early Universe, as pointed out for example by Buchhave et al. (2012), and Zakrisson et al. (2016).

### 3.3. The P-M correlation is dependent on the stellar spectral type

We show in Fig. 9 the same data but with stars of F, G and K spectral types color-coded in red, blue and black symbols, respectively, both in the scatter plot and in the average trend (the filled circles with error bars). It is clear that F and G-type stars behave quite similar, while K-type stars are different, in the sense that they have higher ( $\sim 2\sigma$ )  $\Delta[\text{Fe}/\text{H}]$  for SWNPs (the fourth bin in Fig. 9), and are marginally (about or slightly less than  $1\sigma$ ) higher for SWEs (the second and third bins). If the observed difference is real, we argue that it might originate from the different convective zones in the scenario of pollution, or is due to different mass of proto-planetary disk in the scenario of core-accretion scenario. This is consistent with the implication presented by the approach of the solid and dashed line in the high mass end in the middle panel of Fig. 2 in Johnson et al. (2010), which hints for a decreasing  $\Delta[\text{Fe}/\text{H}]$  with stellar mass increasing.

Stellar models have been constructed by Pinsonneault et al. (2001) to estimate the mass of the outer convective zone in FGK main sequence (MS) stars, and the mass of convective zone is found to decrease dramatically with stellar mass, and any contamination of a star's atmosphere by accreted planetary material should affect hotter stars much more than cool stars. This trend is not observed in this plot, however. In fact, the trend shown in this plot is contrary to this prediction and therefore it strongly rejects the pollution scenario for the P-M correlation. In addition, the significant high metallicity of K-type SWPs with  $R_{\text{P}} > 3R_{\oplus}$  suggest that K stars require much higher content of metals to form large planets in their discs than FG stars, which can be naturally explained by the core-accretion model as less massive disk needs more metals to form a rock core more massive than approximately  $10 M_{\oplus}$ .

In addition, we show in the upper portion of Fig. 9 in units of percentage the ratios of the number of stars in each radius bin of a certain spectral type to the total number of stars of the same spectral type. It is clear and quite interesting as shown that F and G-type stars again have similar distributions, while K-type stars are significantly less frequent for Earth-sized planets, and turns to be more frequent at Neptune-sized planets. We will discuss the difference in the occurrence rate for SWPs of different spectral types in our next work (Wang et al. *in prep.*), and in this paper the distributions are only used to exclude the possibility that the differences in metal enhancement pattern for FG-type stars and K-type stars result from the differences in frequencies, because they (the solid and

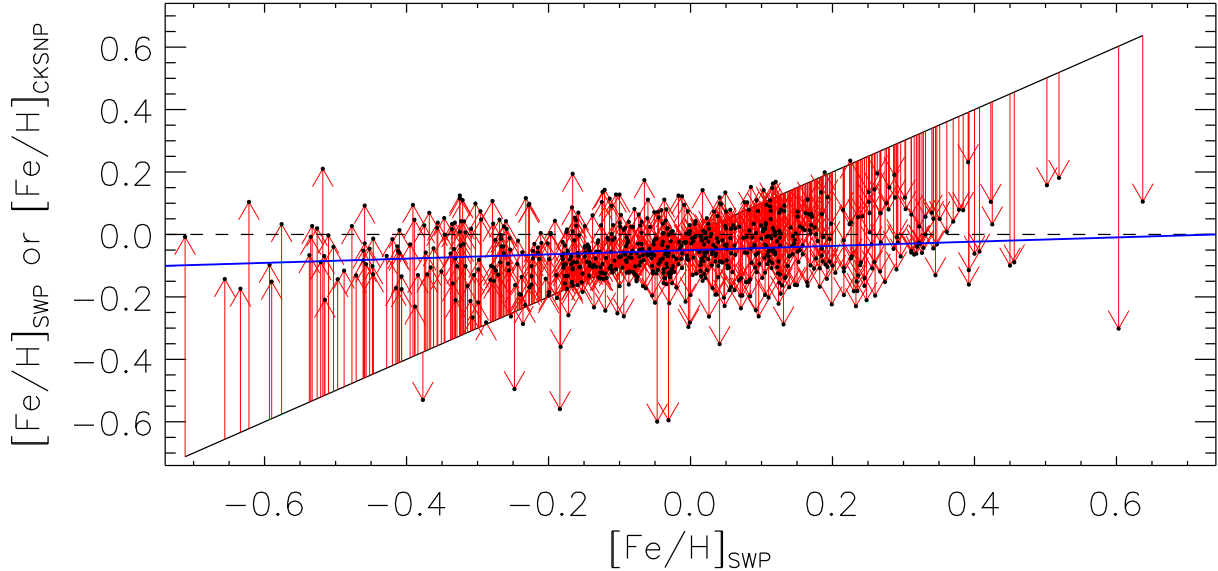


**Figure 8.**  $[\text{Fe}/\text{H}]_{\text{SWP}}$  (black line) and  $[\text{Fe}/\text{H}]_{\text{CKSNP}}$  (black dots) against  $[\text{Fe}/\text{H}]_{\text{SWP}}$ . The arrows show the directions from  $[\text{Fe}/\text{H}]_{\text{SWP}}$  to  $[\text{Fe}/\text{H}]_{\text{CKSNP}}$  for each pair. The blue straight line is the best linear fit to  $[\text{Fe}/\text{H}]_{\text{CKSNP}}$  against  $[\text{Fe}/\text{H}]_{\text{SWP}}$ .

broken lines) have quite different trends. We note that the numbers of SWPs of F, G and K-spectral types are 329, 336 and 73, respectively. This is the main reason that the overall trend for the entire sample (the cyan lines) follow those of F and G SWPs (the red and blue curves).

#### 4. CONCLUSION

We employ the LMDR3 stellar spectral library with the Kepler planet candidates to create the largest samples of stars with planets in a relatively restricted volume in the Milky Way, and a well-defined sample of stars with no planets, with which we perform detailed investigations of the P-M correlation. We firstly point out that the selection of the control sample (the SNP sample) is very crucial, given that most of them are in the Milky way which shows metallicity gradient, and therefore stars at different positions inherently contain different metallicities. We show that with control samples averagely further away from us comparing to the target sample (the SWP sample), they have less metallicities gradually. For our study, by constraining the  $T_{\text{eff}}$ ,  $\log g$ ,  $r$  magnitude and  $g-r$  color of the SNPs to be close to those of the SWPs, the comparison pair should have similar stellar properties (excluding metallicities) and distances from the Sun. We believe our selected control sample is the best for such kind of statistical studies.

We find that in general SWPs are more metal-rich than SNPs, but due to the fact that most of our SWPs' planets are Earth- Size or Neptune-size, and the extent of the over-metallicity of our SWP sample as compared to the SNP sample is not significant. We confirm that the P-M correlation, or the higher-metallicity of SWPs compared to SNPs, is

strong for SWJPs, and weaker for SWNPs, and become only marginal for SWEs and SWMPs (star with massive planets). In other words, we find for the first time a clear peak of  $\Delta[\text{Fe}/\text{H}]$  at Jupiter-sized planets. In addition, the percentage of stars with  $\Delta[\text{Fe}/\text{H}] > 0$  has a similar trend. Based on this turn-over trend, we believe that the mechanism of giant planets formation might be different from both rocky planets and very massive planets or brown dwarfs, so they should not form through only core-collapse or solely through collisional growth of planet embryos.

We also find it obvious that FG type stars follow this general trend, but K stars are slightly different in the sense that obvious metal enhancement ( $\sim 0.1-0.2$  dex) is detected for stars bearing Neptunian-sized planets and Super-Earths as compared to SNPs, which indicates that much higher metallicities are required for Neptunes and Super-Earths to form around K type stars, than those around FG stars.

We point out for the first time that the P-M correlation is also dependent on stellar metallicities, i.e., we observe positive  $\Delta[\text{Fe}/\text{H}]$  at solar or super-solar metallicities, and negative  $\Delta[\text{Fe}/\text{H}]$  at subsolar metallicities. The dependence may be mathematically explained by the fact the SWPs has a metallicity deviation about twice of SNPs', and there when  $[\text{Fe}/\text{H}]_{\text{SWPs}}$  increases or decreases,  $\Delta[\text{Fe}/\text{H}]$  increases and decreases accordingly, but with a slightly less extent.

To summary, we conclude that giant planets probably form differently from rocky planets or more massive planets/brown dwarfs, and the core-accretion scenario is highly favored by our result. No steady increase of  $\Delta[\text{Fe}/\text{H}]$  within error bars against planet sizes is observed for stars with rocky planets, which could rule out the metal pollution theory for

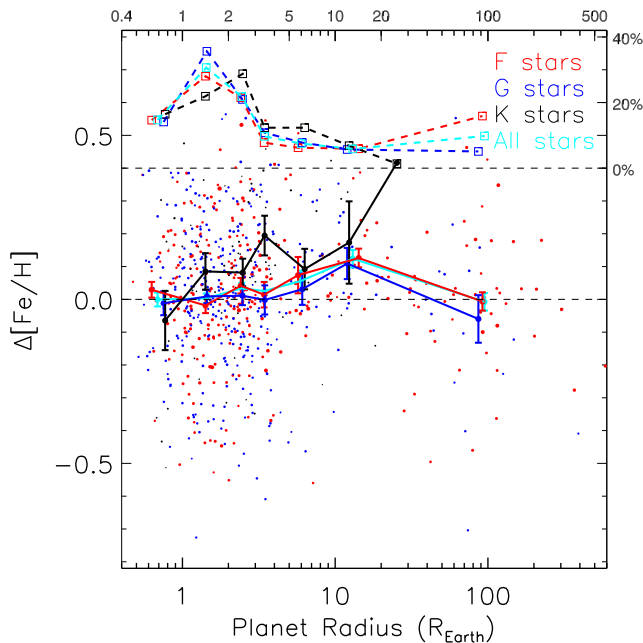


**Figure 9.** Same data and same labels as Fig.6, but with stars of F, G, K and all spectral type differentially colored in red, blue, black and cyan, respectively. The connected filled circles with error bars are the mean values and standard errors in the same  $R_P$  bins. The most right black dot does not have error bar because there is only one object in this bin for K stars. For each spectral type from F to K, the fractions of stars in each  $R_P$  bin with respect to the total number of stars in each spectral type are shown as open squares connected by dashed lines with the same color coding as in the upper part of the plot. The upper horizontal dashed line represents where the fractions equal zero percent, while the lower one represents where  $\Delta[\text{Fe}/\text{H}]$  equals zero.

the apparent P-M correlation, because massive rocky planets should also be able to contribute a large amount of metals into stellar photospheres if engulfed. Instead, this observation implies a higher metallicity is prerequisite for massive planets to form.

This research is supported by the National Natural Science Foundation of China (NSFC) under grants No. 11203035 and 11390371, and is accomplished (in part) by the Chinese Academy of Sciences (CAS), through a grant to the CAS South America Center for Astronomy (CASSACA) in Santiago, Chile. Y.Q.C. acknowledges support from NSFC grant No.11625313.

The Guoshoujing Telescope (the Large Sky Area Multi-Object Fiber Spectroscopic Telescope, LAMOST) is a National Major Scientific Project built by the Chinese Academy of Sciences. Funding for the project has been provided by the National Development and Reform Commission. LAMOST is operated and managed by the National Astronomical Observatories, Chinese Academy of Sciences.

## REFERENCES

- Adibekyan, V. Z., Sousa, S. G., Santos, N. C., Delgado Mena, E., González Hernández, J. I., Israelian, G., Mayor, M., & Khachatryan, G. 2012, *A&A*, 545, A32
- Batalha, N. M., et al. 2013, *ApJS*, 204, 24
- Borucki, W. J., et al. 2011, *ApJ*, 736, 19
- Bouchy, F., et al. 2009, *A&A*, 496, 527
- Brown, T. M., Latham, D. W., Everett, M. E., & Esquerdo, G. A. 2011, *AJ*, 142, 112
- Bruntt, H., et al. 2012, *MNRAS*, 423, 122
- Buchhave, L. A., & Latham, D. W. 2015, *ApJ*, 808, 187
- Buchhave, L. A., et al. 2012, *Nature*, 486, 375
- . 2014, *Nature*, 509, 593
- Burke, C. J., Bryson, S., Christiansen, J., Mullally, F., Rowe, J., Science Office, K., & Kepler Science Team. 2013, in *American Astronomical Society Meeting Abstracts*, Vol. 221, American Astronomical Society Meeting Abstracts, 216.02
- Catanzarite, J., & Shao, M. 2011, *ApJ*, 738, 151
- Chaplin, W. J., et al. 2014, *ApJS*, 210, 1
- Coelho, P., Barbuy, B., Meléndez, J., Schiavon, R. P., & Castilho, B. V. 2005, *A&A*, 443, 735
- Cui, X.-Q., et al. 2012, *Research in Astronomy and Astrophysics*, 12, 1197
- De Cat, P., et al. 2015, *ApJS*, 220, 19
- Deng, L.-C., et al. 2012, *Research in Astronomy and Astrophysics*, 12, 735
- Dong, S., Xie, J.-W., Zhou, J.-L., Zheng, Z., & Luo, A. 2018, *Proceedings of the National Academy of Science*, 115, 266
- Dong, S., et al. 2014, *ApJL*, 789, L3
- Dressing, C. D., & Charbonneau, D. 2013, *ApJ*, 767, 95
- Ercolano, B., & Clarke, C. J. 2010, *MNRAS*, 402, 2735
- Everett, M. E., Howell, S. B., Silva, D. R., & Szkody, P. 2013, *ApJ*, 771, 107

- Fischer, D. A., & Valenti, J. 2005, *ApJ*, 622, 1102
- Fressin, F., et al. 2013, *ApJ*, 766, 81
- Ghezzi, L., Cunha, K., Schuler, S. C., & Smith, V. V. 2010, *ApJ*, 725, 721
- Gonzalez, G. 1997, *MNRAS*, 285, 403
- Gonzalez, G., Brownlee, D., & Ward, P. 2001, *Icarus*, 152, 185
- Han, E., Wang, S. X., Wright, J. T., Feng, Y. K., Zhao, M., Fakhouri, O., Brown, J. I., & Hancock, C. 2014, *PASP*, 126, 827
- Howard, A. W., et al. 2012, *ApJS*, 201, 15
- Ida, S., & Lin, D. N. C. 2004, *ApJ*, 616, 567
- . 2005, *ApJ*, 626, 1045
- Johnson, J. A., Aller, K. M., Howard, A. W., & Crepp, J. R. 2010, *PASP*, 122, 905
- Lin, D. N. C., Bodenheimer, P., & Richardson, D. C. 1996, *Nature*, 380, 606
- Lissauer, J. J., et al. 2012, *ApJ*, 750, 112
- Luo, A.-L., et al. 2012, *Research in Astronomy and Astrophysics*, 12, 1243
- Marcy, G. W., et al. 2014, *ApJS*, 210, 20
- Molenda-Żakowicz, J., et al. 2013, *MNRAS*, 434, 1422
- Morton, T. D., Bryson, S. T., Coughlin, J. L., Rowe, J. F., Ravichandran, G., Petigura, E. A., Haas, M. R., & Batalha, N. M. 2016, *ApJ*, 822, 86
- Morton, T. D., & Johnson, J. A. 2011, *ApJ*, 738, 170
- Mulders, G. D., Pascucci, I., Apai, D., Frasca, A., & Molenda-Żakowicz, J. 2016, *AJ*, 152, 187
- Murray, N., & Chaboyer, B. 2002, *ApJ*, 566, 442
- Murray, N., Paskowitz, M., & Holman, M. 2002, *ApJ*, 565, 608
- Neves, V., Bonfils, X., Santos, N. C., Delfosse, X., Forveille, T., Allard, F., & Udry, S. 2013, *A&A*, 551, A36
- Pinsonneault, M. H., DePoy, D. L., & Coffee, M. 2001, *ApJL*, 556, L59
- Santerne, A., et al. 2012, *A&A*, 545, A76
- Schlaufman, K. C. 2015, *ApJL*, 799, L26
- Soderblom, D. R., & King, J. R. 1998, in *Solar Analogs: Characteristics and Optimum Candidates.*, ed. J. C. Hall, 41
- Sousa, S. G., Santos, N. C., Israelian, G., Mayor, M., & Udry, S. 2011, *A&A*, 533, A141
- Sousa, S. G., et al. 2008, *A&A*, 487, 373
- Thygesen, A. O., et al. 2012, *A&A*, 543, A160
- Wang, J., & Fischer, D. A. 2013, *ArXiv e-prints*
- . 2015, *AJ*, 149, 14
- Wang, L., et al. 2016, *AJ*, 152, 6
- Wu, Y., Du, B., Luo, A., Zhao, Y., & Yuan, H. 2014, in *IAU Symposium, Vol. 306, Statistical Challenges in 21st Century Cosmology*, ed. A. Heavens, J.-L. Starck, & A. Krone-Martins, 340–342
- Wu, Y., et al. 2011, *Research in Astronomy and Astrophysics*, 11, 924
- Zackrisson, E., Calissendorff, P., González, J., Benson, A., Johansen, A., & Janson, M. 2016, *ApJ*, 833, 214
- Zhao, G., Zhao, Y.-H., Chu, Y.-Q., Jing, Y.-P., & Deng, L.-C. 2012, *Research in Astronomy and Astrophysics*, 12, 723